
ParallelTime: Dynamically Weighting the Balance of Short- and Long-Term Temporal Dependencies

Itay Katav

Department of Computer Science
Ben-Gurion University of the Negev
Beer Sheva, Israel
katavit@post.bgu.ac.il

Aryeh Kontorovich

Department of Computer Science
Ben-Gurion University of the Negev
Beer Sheva, Israel
karyeh@cs.bgu.ac.il

Abstract

Modern multivariate time series forecasting primarily relies on two architectures: the Transformer with attention mechanism and Mamba. In natural language processing, an approach has been used that combines local window attention for capturing short-term dependencies and Mamba for capturing long-term dependencies, with their outputs averaged to assign equal weight to both. We find that for time-series forecasting tasks, assigning equal weight to long-term and short-term dependencies is not optimal. To mitigate this, we propose a dynamic weighting mechanism, ParallelTime Weighter, which calculates interdependent weights for long-term and short-term dependencies for each token based on the input and the model’s knowledge. Furthermore, we introduce the ParallelTime architecture, which incorporates the ParallelTime Weighter mechanism to deliver state-of-the-art performance across diverse benchmarks. Our architecture demonstrates robustness, achieves lower FLOPs, requires fewer parameters, scales effectively to longer prediction horizons, and significantly outperforms existing methods. These advances highlight a promising path for future developments of parallel Attention-Mamba in time series forecasting. The implementation is readily available at: [ParallelTime GitHub](#).

1 Introduction

Forecasting is one of the most important tasks in time series analysis. To address this challenge, various architectures have been proposed. The Transformer architecture [Vaswani et al., 2017], which has achieved remarkable success in natural language processing [Brown et al., 2020] and computer vision [Dosovitskiy et al., 2021], has also shown promise in time series forecasting [Nie et al., 2023]. Another successful architecture introduced in recent years is the State Space Model (SSM) [Gu et al., 2022, Smith et al., 2023]. SSM-based models, such as Mamba [Gu and Dao, 2023], have demonstrated strong performance in time series forecasting [Wang et al., 2024] and other domains.

Each approach has its distinct advantages. Mamba, through its parameter initialization, produces a summary of long-term dependencies [Gu et al., 2020]. The latter allows for extraction of the leading features for forecasting, while filtering out the noise in the time series. Attention models, such as the transformer, are highly accurate and excel at capturing complex patterns and interactions across the sequence, enabling robust forecasting performance [Nie et al., 2023]. Moreover, in cases of channel independence, where each variable in a multivariate time series is processed separately using the same model weights, attention models demonstrate superior performance on datasets with similar variates series [Nie et al., 2023]. In contrast, Mamba models, such as those proposed in Wang et al. [2024], achieve better results on datasets with heterogeneous variates series.

In this paper, we propose a novel method that combines the strengths of Mamba and the attention mechanism by computing both Mamba, which captures long-term dependencies, and a small local window attention, which focuses on short-term dependencies. Recent papers in natural language processing [Dong et al., 2024] tackle this problem by computing the mean of the values and assigning equal weight to both components. In contradistinction, our approach weights each component of each token separately. In cases where more long-range dependencies are needed for the prediction, the ParallelTime Weighter gives more weight to the Mamba component. When more short-term dependency predictions are required, more weight is given to the window attention component. Additionally, we leverage registers as domain-specific global context, providing a persistent reference that captures information beyond the input series. We demonstrate that our method is robust and significantly outperforms existing approaches, on almost every benchmark dataset.

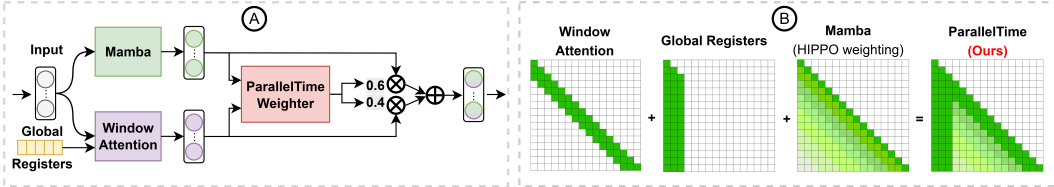


Figure 1: (A) High level visualization of ParallelTime module. (B) Diagram of the attention map of ParallelTime, integrating global registers, local window attention, and Mamba components.

Our contributions. The main contributions of this paper are three-fold:

- We propose a novel ParallelTime Weighter that selects the contributions of short-term, long-term, and global memory for each time series patch, implemented via window-based attention, Mamba, and registers, respectively, to improve the accuracy of long-term forecasting.
- We demonstrate that parallel Mamba-Attention architecture is currently the most effective approach for long-term time series forecasting, highlighting a promising direction for future advancements in time series forecasting models.
- Our model, ParallelTime, achieves SOTA performance on real-world benchmarks, delivering better results from previews models with fewer parameters and lower computational cost, a characteristic highly critical for real-time forecasting applications.

2 Related Work

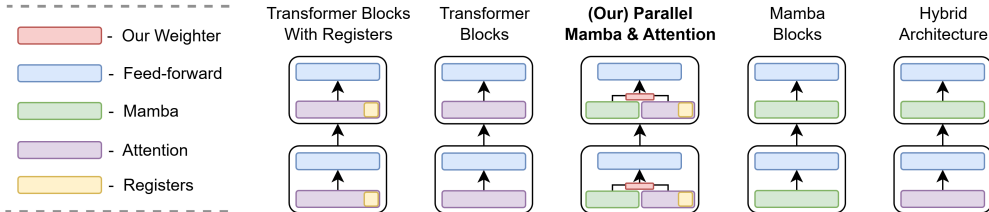


Figure 2: Comparison of five neural network block architectures: Transformer Blocks with Registers, Transformer Blocks, (Ours) Parallel Mamba-Attention with dynamic weighting mechanism, Mamba Blocks, and Hybrid Sequential Mamba-Attention Architecture.

Transformer Vaswani et al. [2017], leveraging causal self-attention layers and feed-forward networks, has laid a powerful foundation for time series forecasting [Zhou et al., 2021, 2022]. A standout example is PatchTST [Nie et al., 2023], which achieves SOTA performance by utilizing channel independence to process each variable in a multivariate time series separately. By feeding contiguous time series patches as tokens into a standard self-attention mechanism, PatchTST outperforms many previous models. In standard self-attention, each token attends to all preceding tokens to capture global dependencies. To focus on local patterns, windowed attention variants, such as those in

LongFormer [Beltagy et al., 2020a] and Swin Transformer [Liu et al., 2021], restrict each token to attend only to the most recent S tokens, as illustrated in Figure 1 (B).

Registers are model parameters that function as tokens, concatenated with input tokens to provide additional global domain-specific information. They serve as a persistent reference for the model, capturing information not explicitly present in the input tokens. Registers have shown considerable promise in natural language processing, as demonstrated by Burtsev et al. [2020], and in computer vision, as explored by Darcet et al. [2024], where they enhance model performance by leveraging task-specific memory.

Mamba [Gu and Dao, 2023] is a State Space Model (SSM) [Gu et al., 2022, Smith et al., 2023] designed for efficient [Waleffe et al., 2024] and high-performance sequence modeling. At the core of the Mamba architecture is the HIPPO matrix [Gu et al., 2020], which prioritizes recent tokens by assigning them greater influence in the state representation while compressing older tokens into a compact, approximated summary. This approach effectively captures a condensed representation of long-range dependencies, making it well-suited for time series forecasting. S-Mamba [Wang et al., 2024] has demonstrated competitive performance across several time series forecasting benchmarks.

Hybrid models which combine Mamba and Attention layers in a sequential stack, have gained prominence in natural language processing, as demonstrated by models such as Jamba [Team et al., 2024] and Samba [Ren et al., 2024]. In time-series forecasting, Heracles [Patro et al., 2024] showcases the versatility and effectiveness of this approach. However, sequential stacking may introduce information bottlenecks [Dong et al., 2024] and poses challenges in determining the optimal placement of each component, potentially compromising forecasting accuracy.

Parallel architectures where Mamba and attention mechanisms process the same input simultaneously and their outputs are combined in some way, have recently been proposed in natural language processing. For instance, Hymba [Dong et al., 2024] proposed aggregating Mamba and attention outputs via simple averaging. However, in time series forecasting, where window attention mechanisms capture short-term dependencies at each layer, and Mamba is responsible for summarizing long-term dependencies, assigning equal weights to both long-term and short-term dependencies may not optimally capture the right amount of each dependency needed for each prediction, especially when time series variates differ significantly. To the best of our knowledge, no prior work has applied parallel Mamba-Attention models to long-term time series forecasting. We demonstrate that our novel weighted aggregation approach, ParallelTime Weighter, outperforms naive combinations, leveraging the strengths of both components to achieve state-of-the-art performance.

3 ParallelTime

Problem definition. In multivariate long-term time series forecasting, the task is to predict future values of multiple interdependent variables based on historical data. Given a multivariate time series $\mathbf{X} = (\mathbf{x}_1, \dots, \mathbf{x}_T) \in \mathbb{R}^{N \times T}$, where N is the number of variables and T is the number of timestamps, the goal is to forecast H future values $\mathbf{Y} = (\mathbf{x}_{T+1}, \dots, \mathbf{x}_{T+H}) \in \mathbb{R}^{N \times H}$. Each $\mathbf{x}_t \in \mathbb{R}^N$ represents the observations of N variables at time t .

3.1 Overall Architecture

The ParallelTime architecture is illustrated in Figure 3. Our model begins by decomposing the multivariate time series input into N univariate series, leveraging the channel independence framework [Nie et al., 2023]. This approach enables all model weights to learn more than one variant, enhancing robustness during testing. To address distribution shifts across different time series, we apply instance normalization (ReVIN) [Kim et al., 2022] to the input. Subsequently, a patching mechanism divides each univariate series into non-overlapping patches, treating each patch as a "token" with features derived from the univariate time series values. We tried overlapping patches, but they increased computational cost without improving accuracy, so they were not used.

To effectively extract both global trend and local trends from each patch, we employ a dual embedding strategy. A linear layer aggregates global information by mixing all data points within the patch, while a Conv1D layer [O’Shea and Nash, 2015] captures local trends within the patch. The global and local representations are then combined through summation to form the final \mathbf{x}_e patch embedding.

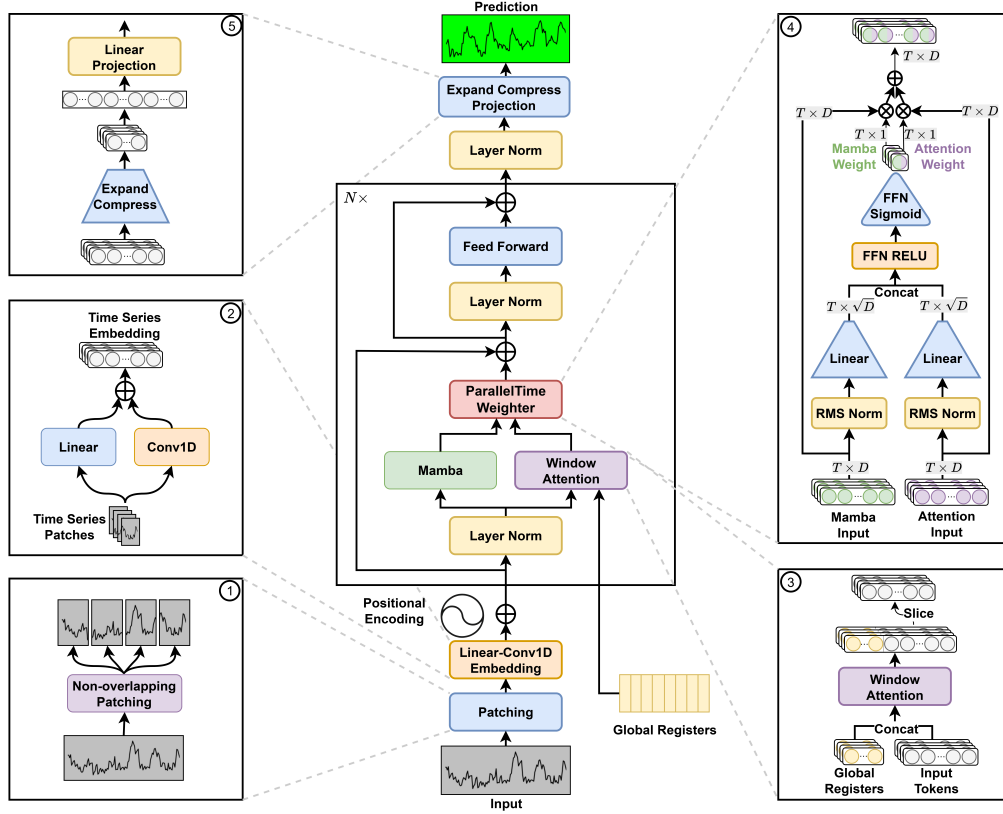


Figure 3: The architecture of ParallelTime. The input time series ① is sliced into non-overlapping patches. ② Each patch is embedded and augmented with positional encoding. The resulting tokens are processed through N stacked ParallelTime blocks. Each block first normalizes the input, tokens Mamba computation and ③ windowed attention with a register in parallel, ④ weights their outputs using a ParallelTime Weighter mechanism, and then applies normalization followed by a nonlinear feedforward layer. Finally, the output is normalized ⑤ and processed through an expand-compress-projection mechanism to generate the horizon prediction.

To capture sequential order in attention models, which function as a bag of words without positional encoding [Vaswani et al., 2017], we incorporate absolute positional encoding, defined as $\mathbf{x}_d = \mathbf{x}_e + \mathbf{x}_{pos} \in \mathbb{R}^{P \times dim}$, where \mathbf{x}_e represents the input embedding, \mathbf{x}_{pos} denotes the positional encoding, and \mathbf{x}_d is the resulting encoded representation.

3.2 ParallelTime Decoder Block

Our approach builds upon a decoder-only transformer architecture [Vaswani et al., 2017] As illustrated in Figure 3, the decoder is composed of a stack of N identical layers, with each layer comprising two sublayers. The first sublayer integrates parallel Mamba and attention mechanisms, with their outputs processed by the ParallelTime Weighter, which dynamically allocates weights to the Mamba and attention outputs for each patch or token. The second sublayer is a non-linear feed-forward network with SiLU activation. Each sublayer begins with LayerNorm [Ba et al., 2016] and is enclosed by residual connections [He et al., 2016].

3.3 Mamba and Windowed Attention with Global Registers

Mamba mechanism. To achieve high accuracy with low memory requirements, we added a Mamba block [Gu and Dao, 2023], which leverages a state-space model. Mamba’s strength lies in its high accuracy [Wang et al., 2024] and constant memory usage, making it ideal for long time series

forecasting. The core operation of Mamba is defined as:

$$\mathbf{h}_t = \mathbf{A}\mathbf{h}_{t-1} + \mathbf{B}\mathbf{x}_t, \quad \mathbf{y}_t = \mathbf{C}\mathbf{h}_t,$$

where $\mathbf{x}_t \in \mathbb{R}^{dim}$ is the input at time t , $\mathbf{h}_t \in \mathbb{R}^{dim}$ is the hidden state, and $\mathbf{A}, \mathbf{B}, \mathbf{C}$ are learnable parameters of the state-space model. The output:

$$\mathbf{x}_{mamba} = \text{Mamba}(\mathbf{x}_d),$$

effectively captures long-range dependencies in the input sequence $\mathbf{x}_d \in \mathbb{R}^{P \times dim}$.

Windowed Attention Mechanism. To capture local interactions efficiently within each layer, we utilize a causal multi-head windowed self-attention mechanism Beltagy et al. [2020b]. This approach allows us to restrict attention to a fixed window. We select a small window size, set at a 1 : 9 ratio relative to the number of input sequence patches, ensuring that the attention mechanism focuses solely on short-term dependencies while delegating long-term dependencies to Mamba.

Global Registers. To incorporate global context, we introduce global register tokens, denoted as $\mathbf{W}_{reg} \in \mathbb{R}^{R \times dim}$, where R is the number of registers and dim is the embedding dimension. These tokens serve as a compact repository of domain-specific global information, providing the model with access to broader contextual cues. The input sequence $\mathbf{x}_d \in \mathbb{R}^{P \times dim}$, is concatenated with the global registers to form: $\mathbf{x}_{cat} = \text{Concat}(\mathbf{W}_{reg}, \mathbf{x}_d) \in \mathbb{R}^{(R+P) \times dim}$. This concatenated sequence is then processed by the causal multi-head windowed attention mechanism, yielding:

$$\mathbf{x}_{att} = \text{WinAtt}(\mathbf{x}_{cat}).$$

3.4 ParallelTime Weighter

Considering the Mamba \mathbf{x}_{mamba} , which encapsulates both short-term and long-term dependencies, and the window attention \mathbf{x}_{att} , which reflects short-term dependencies alongside global dependencies obtained from the registers, to make accurate prediction for different inputs, some inputs need to have more long-term dependency and some need more global, and short-term dependencies, giving a weight to each representation isn't enough, we want the weights to be in respect to each other, so we created the novel ParallelTime Weighter.

The attention and Mamba outputs, \mathbf{x}_{att} and \mathbf{x}_{mamba} , are first normalized using RMSNorm [Zhang and Sennrich, 2019] to address their differing scales. Each output is then processed by a dedicated linear transformation that compresses the dimensionality from dim to \sqrt{dim} , preserving essential features:

$$\mathbf{x}'_{att} = \text{RMSNorm}(\mathbf{x}_{att})\mathbf{W}_{att} \in \mathbb{R}^{P \times \sqrt{dim}},$$

$$\mathbf{x}'_{mamba} = \text{RMSNorm}(\mathbf{x}_{mamba})\mathbf{W}_{mamba} \in \mathbb{R}^{P \times \sqrt{dim}}.$$

These specialized linear layers effectively tailor the compression to the unique characteristics of the attention and Mamba outputs. The compressed representations are then concatenated to form a unified feature set:

$$\mathbf{x}'_{cat} = \text{Concat}(\mathbf{x}'_{att}, \mathbf{x}'_{mamba}) \in \mathbb{R}^{P \times 2\sqrt{dim}},$$

Following concatenation, the compressed features from the attention and Mamba branches are processed through a two-layer transformation to capture complex interactions. Inspired by the kernel trick [Hearst et al., 1998], this approach leverages higher-dimensional spaces to reveal patterns not readily discernible in lower dimensions, this step generates adaptive weights:

$$\mathbf{x}_{weights} = \sigma(\text{ReLU}(\mathbf{x}'_{cat}\mathbf{W}_1)\mathbf{W}_2) \in \mathbb{R}^{P \times 2}, \mathbf{W}_1 \in \mathbb{R}^{2\sqrt{dim} \times dim-h}, \mathbf{W}_2 \in \mathbb{R}^{dim-h \times 2}$$

where $dim-h$ denotes a dimension higher than $2\sqrt{dim}$, and σ represents the sigmoid function. We attempted to replace the sigmoid function with softmax, but it yielded suboptimal results. This observation aligns with other weight mechanisms, such as the Squeeze-and-Excitation approach [Hu et al., 2018], which also performed better with sigmoid. The weight vector is defined as $\mathbf{x}_{weights} = [\mathbf{x}_{weight}^{att}, \mathbf{x}_{weight}^{mamba}]$. The final output is computed as a weighted sum of the original attention and Mamba outputs:

$$\mathbf{x}_{out} = \mathbf{x}_{att} \cdot \mathbf{x}_{weight}^{att} + \mathbf{x}_{mamba} \cdot \mathbf{x}_{weight}^{mamba},$$

This architecture enables the weights to dynamically balance the contributions of each branch, leading to superior performance, as demonstrated in Table 1.

Following the decoder layers, we apply Layer Normalization (LayerNorm). Unlike standard time series forecasting architectures that simply flatten and project data, our Expand-Compress-Project approach is more efficient. We first expand the data to a higher dimension than the input ($\text{dim} \times \text{higher-dim}$) and then compress it to a significantly smaller dimension ($\text{dim} \div \text{some-dim}$) than the input dimension. This approach reduces millions of parameters while maintaining comparable performance (see Appendix 5 for details). The projection output forms our model’s prediction, which we then de-normalize using ReVIn [Kim et al., 2022].

3.5 Loss and Optimizer

We employed the Huber loss function [Huber, 1992, Wen et al., 2019], chosen for its enhanced robustness to outliers and contribution to improved training stability. The Huber loss is defined as:

$$\mathcal{L}_{\text{huber}}(x_t, \hat{x}_t) = \begin{cases} (x_t - \hat{x}_t)^2 \frac{1}{2}, & \text{if } |x_t - \hat{x}_t| \leq \delta. \\ \delta \times (|x_t - \hat{x}_t| - \frac{1}{2} \times \delta), & \text{else.} \end{cases} \quad (1)$$

where x_t is the true value, \hat{x}_t is the predicted value, and δ is a hyperparameter modulating the balance between L1 and L2 loss characteristics.

For optimization, we used the Adam optimizer [Kingma and Ba, 2015], which provides efficient adaptive learning rate adjustments. Further details regarding the training process and specific hyperparameter settings can be found in Appendix 8.2.

4 Evaluations

4.1 Baselines and Experimental Setup

To assess the performance of our proposed ParallelTime, we compare it against several SOTA models for long time series forecasting. These include Transformer-based models such as PatchTST [Nie et al., 2023] and FEDFormer [Zhou et al., 2022], Linear models like DLinear [Zeng et al., 2023] and N-BEATS [Oreshkin et al., 2020], foundational models including Moment [Goswami et al., 2024], GPT4TS [Zhou et al., 2023], and TimesNet [Wu et al., 2023], as well as ensemble models LightTS [Campos et al., 2023] and Stationary. We evaluate all models on eight widely used datasets: Electricity, Weather, Illness, Traffic, and four ETT datasets (ETTh1, ETTh2, ETTm1, ETTm2). For detailed dataset descriptions, see Appendix 8.1.

We adopt standard evaluation protocols with prediction horizons of $T \in \{24, 36, 48, 60\}$ for the Illness dataset and $T \in \{96, 192, 336, 720\}$ for all other datasets. Performance metrics for baseline models are obtained from Goswami et al. [2024], while our model’s results are newly computed. A look-back window of $L = 512$ is used for all models, except DLinear, which employs an optimized input length of $L = 96$ to enhance performance.

4.2 Main Results

Comprehensive forecasting results are listed in Table 1, with the best performance highlighted in **red** and the second best underlined. A lower Mean Squared Error (MSE) and Mean Absolute Error (MAE) indicate more accurate predictions. Our proposed model, ParallelTime, demonstrates exceptional performance across a diverse set of datasets and prediction horizons, consistently outperforming a range of state-of-the-art models, ParallelTime achieves the best forecasting accuracy in a significant number of scenarios, particularly excelling in datasets such as Weather, ETTh1, ETTh2, ETTm2, Electricity, Traffic, and Illness.

Our model, ParallelTime, surpasses SOTA models, including PatchTST [Nie et al., 2023] and Moment [Goswami et al., 2024], in long-term time series forecasting. Although PatchTST remains a strong contender, ranking as the second-best performer, and Moment excels on the ETTm2 dataset (likely due to its training data), ParallelTime achieves superior performance with significantly fewer parameters and lower computational complexity, compared to PatchTST (see Table 2). Specifically, ParallelTime reduces MSE by an average of 4.25% and MAE by 4.31% relative to PatchTST. This

Methods Metric	ParallelTime		MOMENT		GPT4TS		PatchTST		DLinear		TimesNet		FEDFormer		Stationary		LightTS		N-BEATS		
	MSE	MAE	MSE	MAE	MSE	MAE	MSE	MAE	MSE	MAE	MSE	MAE									
Weather	96	0.145	0.189	0.154	0.209	0.162	0.212	<u>0.149</u>	<u>0.198</u>	0.176	0.237	0.172	0.220	0.217	0.296	0.173	0.223	0.182	0.242	0.152	0.210
	192	0.189	0.232	0.197	0.248	0.204	0.248	<u>0.194</u>	<u>0.241</u>	0.220	0.282	0.219	0.261	0.276	0.336	0.245	0.285	0.227	0.287	0.199	0.260
	336	0.242	0.273	0.246	0.285	0.254	0.286	<u>0.245</u>	<u>0.282</u>	0.265	0.319	0.280	0.306	0.339	0.380	0.321	0.338	0.282	0.334	0.258	0.311
	720	0.323	0.331	<u>0.315</u>	0.336	0.326	0.337	0.314	0.334	0.333	0.362	0.365	0.359	0.403	0.428	0.414	0.410	0.352	0.386	0.331	0.359
ETTh1	96	0.365	<u>0.398</u>	0.387	0.410	0.376	0.397	<u>0.370</u>	0.399	0.375	0.399	0.384	0.402	0.376	0.419	0.513	0.491	0.424	0.432	0.399	0.428
	192	0.399	0.415	0.410	0.426	0.416	0.418	0.413	0.421	<u>0.405</u>	<u>0.416</u>	0.436	0.429	0.420	0.448	0.534	0.504	0.475	0.462	0.451	0.464
	336	0.385	0.414	0.422	0.437	0.442	<u>0.433</u>	<u>0.422</u>	0.436	0.439	0.443	0.491	0.469	0.459	0.465	0.588	0.535	0.518	0.488	0.498	0.500
	720	0.420	0.443	0.454	0.472	0.477	<u>0.456</u>	<u>0.447</u>	0.466	0.472	0.490	0.521	0.500	0.506	0.507	0.643	0.616	0.547	0.533	0.608	0.573
ETTh2	96	0.262	0.328	0.288	0.345	0.285	0.342	<u>0.274</u>	<u>0.336</u>	0.289	0.353	0.340	0.374	0.358	0.397	0.476	0.458	0.397	0.437	0.327	0.387
	192	0.322	0.368	0.349	0.386	0.354	0.389	<u>0.339</u>	<u>0.379</u>	0.383	0.418	0.402	0.414	0.429	0.439	0.512	0.493	0.520	0.504	0.400	0.435
	336	0.312	0.370	0.369	0.408	0.373	0.407	<u>0.329</u>	<u>0.380</u>	0.448	0.465	0.452	0.452	0.496	0.487	0.552	0.551	0.626	0.559	0.747	0.599
	720	<u>0.399</u>	<u>0.434</u>	0.403	0.439	0.406	0.441	0.379	0.422	0.605	0.551	0.462	0.468	0.463	0.474	0.562	0.560	0.863	0.672	1.454	0.847
ETTm1	96	0.284	0.337	0.293	0.349	0.292	0.346	<u>0.290</u>	<u>0.342</u>	0.299	0.343	0.338	0.375	0.379	0.419	0.386	0.398	0.374	0.400	0.318	0.367
	192	<u>0.329</u>	<u>0.366</u>	0.326	0.368	0.332	0.372	0.332	0.369	0.335	0.365	0.374	0.387	0.426	0.441	0.459	0.444	0.400	0.407	0.355	0.391
	336	<u>0.365</u>	0.391	0.352	0.384	0.366	0.394	0.366	0.392	0.369	<u>0.386</u>	0.410	0.411	0.445	0.459	0.495	0.464	0.438	0.438	0.401	0.419
	720	0.424	0.430	0.405	0.416	0.417	0.421	<u>0.416</u>	<u>0.420</u>	0.425	0.421	0.478	0.450	0.543	0.490	0.585	0.516	0.527	0.502	0.448	0.448
ETTm2	96	0.162	0.252	0.170	0.260	0.173	0.262	<u>0.165</u>	<u>0.255</u>	0.167	0.269	0.187	0.267	0.203	0.287	0.192	0.274	0.209	0.308	0.197	0.271
	192	0.218	0.291	0.227	0.297	0.229	0.301	<u>0.220</u>	<u>0.292</u>	0.224	0.303	0.249	0.309	0.269	0.328	0.280	0.339	0.311	0.382	0.285	0.328
	336	0.276	0.327	<u>0.275</u>	<u>0.328</u>	0.286	0.341	0.274	0.329	0.281	0.342	0.321	0.351	0.325	0.366	0.334	0.361	0.442	0.466	0.338	0.366
	720	0.356	0.380	0.363	0.387	0.378	0.401	<u>0.362</u>	<u>0.385</u>	0.397	0.421	0.408	0.403	0.421	0.415	0.417	0.413	0.675	0.587	0.395	0.419
Illness	24	1.166	0.657	2.728	1.114	2.063	0.881	<u>1.319</u>	<u>0.754</u>	2.215	1.081	2.317	0.934	3.228	1.260	2.294	0.945	8.313	2.144	4.539	1.528
	36	1.293	0.727	2.669	1.092	1.868	0.892	<u>1.430</u>	<u>0.834</u>	1.963	0.963	1.972	0.920	2.679	1.080	1.825	0.848	6.631	1.902	4.628	1.534
	48	1.399	0.772	2.728	1.098	1.790	0.884	<u>1.553</u>	<u>0.815</u>	2.130	1.024	2.238	0.940	2.622	1.078	2.010	0.900	7.299	1.982	4.957	1.585
	60	<u>1.615</u>	<u>0.844</u>	2.883	1.126	1.979	0.957	1.470	0.788	2.368	1.096	2.027	0.928	2.857	1.157	2.178	0.963	7.283	1.985	5.429	1.661
Electricity	96	0.128	0.222	0.136	0.233	0.139	0.238	<u>0.129</u>	0.222	0.140	0.237	0.168	0.272	0.193	0.308	0.169	0.273	0.207	0.307	0.131	<u>0.228</u>
	192	0.148	0.240	0.152	0.247	<u>0.153</u>	0.251	0.157	0.240	0.153	0.249	0.184	0.289	0.201	0.315	0.182	0.286	0.213	0.316	<u>0.153</u>	0.248
	336	0.163	0.258	0.167	0.264	0.169	0.266	0.163	<u>0.259</u>	0.169	0.267	0.198	0.300	0.214	0.329	0.200	0.304	0.230	0.333	0.170	0.267
	720	0.197	0.288	0.205	0.295	0.206	0.297	0.197	<u>0.290</u>	0.203	0.301	0.220	0.320	0.246	0.355	0.222	0.321	0.265	0.360	0.208	0.298
Traffic	96	0.349	0.231	0.391	0.282	0.388	0.282	<u>0.360</u>	<u>0.249</u>	0.410	0.282	0.593	0.321	0.587	0.366	0.612	0.338	0.615	0.391	0.375	0.259
	192	0.371	0.240	0.404	0.287	0.407	0.290	<u>0.379</u>	<u>0.256</u>	0.423	0.287	0.617	0.336	0.604	0.373	0.613	0.340	0.601	0.382	0.403	0.274
	336	0.388	0.250	0.414	0.292	0.412	0.294	<u>0.392</u>	<u>0.264</u>	0.436	0.296	0.629	0.336	0.621	0.383	0.618	0.328	0.613	0.386	0.426	0.285
	720	0.429	0.274	0.450	0.310	0.450	0.312	<u>0.432</u>	<u>0.286</u>	0.466	0.315	0.640	0.350	0.626	0.382	0.653	0.355	0.658	0.407	0.508	0.335

Table 1: Full results of in-domain forecasting experiments. A lower MSE or MAE indicates a better prediction. The results obtained from [Goswami et al., 2024]. **Red**: the best, Underline: the 2nd best.

Pred Len	MSE		MAE		Fwd FLOPs		Fwd+Bwd FLOPs		#Params	
	ParallelTime	PatchTST	ParallelTime	PatchTST	ParallelTime	PatchTST	ParallelTime	PatchTST	ParallelTime	PatchTST
96	0.349 (↓3.1%)	0.360	0.231 (↓7.2%)	0.249	8.41G (↓35%)	13.1G	25.2G (↓36%)	39.5G	614k (↓48%)	1194k
192	0.371 (↓2.1%)	0.379	0.240 (↓6.3%)	0.256	8.42G (↓37%)	13.5G	25.2G (↓37%)	40.5G	651k (↓67%)	1980k
336	0.388 (↓1.0%)	0.392	0.250 (↓5.3%)	0.264	8.45G (↓39%)	14.0G	25.3G (↓39%)	42.1G	707k (↓77%)	3160k
720	0.429 (↓0.7%)	0.432	0.274 (↓4.2%)	0.286	8.51G (↓44%)	15.4G	25.5G (↓44%)	46.3G	855k (↓86%)	6306k

Table 2: Comparison of ParallelTime and PatchTST on the Traffic dataset. The table reports MSE, MAE, forward (Fwd) FLOPs (i.e., inference FLOPs), forward and backward (Fwd+Bwd) FLOPs (i.e., training FLOPs), and the number of parameters (#Params). Bold values indicate superior performance. ↓ indicates that lower values are better. The improvement percentages for ParallelTime over PatchTST are shown in parentheses.

combination of high accuracy, computational efficiency, and reduced resource requirements highlights the versatility and effectiveness of ParallelTime, positioning it as a leading solution for real-world time series forecasting challenges.

5 Model Analysis

5.1 Patch-Level Weight Analysis

To illustrate how our model allocates short-term and long-term dependencies for each token (patch), we analyze a sample from the Traffic dataset at prediction lengths of 96 and 192. We extract the weights assigned by our ParallelTime Weighter and present them in Figure 4. Looking at the input and the first block at each prediction length, when the previous patch (from left to right) exhibits

a high value, our model assigns greater weight to Mamba, prioritizing long-term dependencies to reduce overfitting to potential noise. Similarly, in the second block for each prediction length, when consecutive patches are similar, the model leverages Mamba to emphasize long-term dependencies, capturing a broader range of historical behaviors rather than focusing solely on recent patterns. Conversely, when preceding patches differ significantly, the model assigns more weight to the attention mechanism to prioritize short-term dependencies. Notably, for the second blocks, longer prediction lengths exhibit a stronger emphasis on long-term dependencies. For an additional result, see Appendix 9.3.

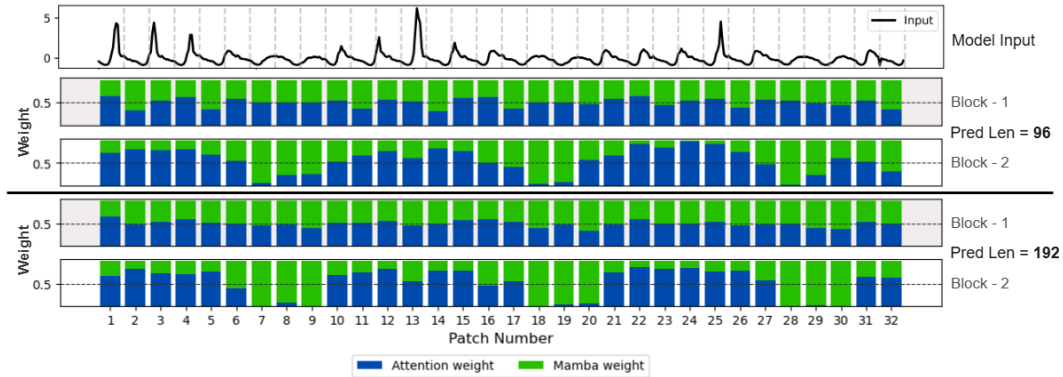


Figure 4: Visualization of input series and the weight distribution for prediction length 96, 192 per patch in sample from Traffic dataset, for each of the first and second ParallelTime blocks.

5.2 Dynamic Weighting Analysis

To evaluate the performance of our dynamic weighting mechanism across various datasets, we computed the mean weight of all tokens (patches) for each layer in our ParallelTime, as shown in Figure 5. The analysis includes the Weather, Electricity, ETTh1, and Traffic datasets.

The results demonstrate that, in the setting where the Attention-Mamba weights of each patch are averaged across all patches, each dataset emphasizes a different balance between short-term and long-term dependencies. Notably, across all datasets, the second layer consistently assigns more weight to the window attention mechanism compared to the first layer. For example, in the Weather dataset, when the prediction lengths are 192 and 336, the model relies more heavily on long-term dependencies, which are captured by the Mamba mechanism in the first layer. Conversely, for prediction lengths of 96 and 720, short-term dependencies are prioritized via the attention mechanism. In the second layer, attention receives a larger share of the weights regardless of the prediction length.

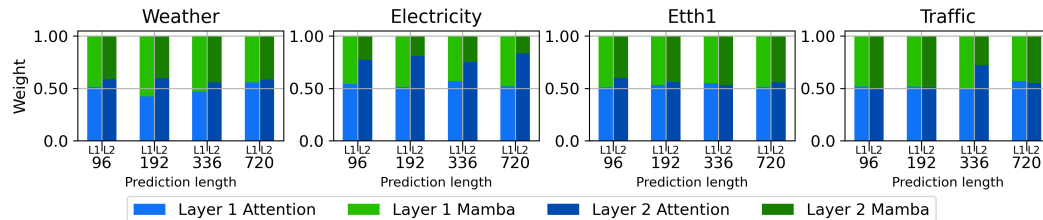


Figure 5: Mean weight of tokens (patches) per layer in the ParallelTime model, highlighting varying requirements for short-term and long-term dependencies across different datasets and prediction horizons.

6 Ablation study

6.1 Weighting Strategy for Attention and Mamba

We assess the impact of our proposed ParallelTime weighting methodology. We compare multiple strategies, including mean weighting, as in [Dong et al., 2024], and sum weighting. To ensure compatibility, Attention and Mamba outputs are normalized prior to weighting to address their differing scales. Our results, as shown in Figure 6, confirm the effectiveness of this approach across all datasets. Additional results for other datasets are provided in Appendix 9.1.

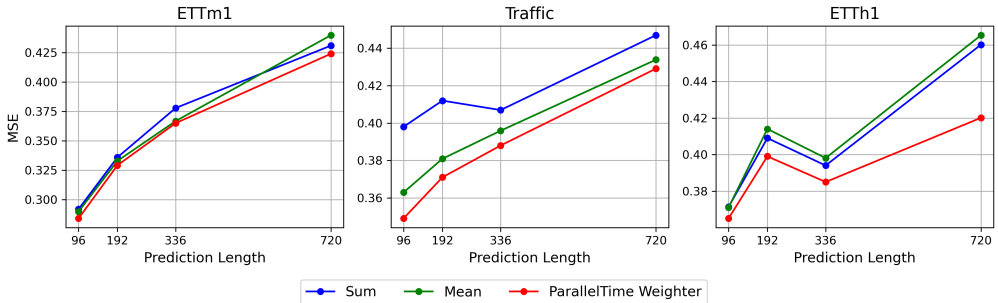


Figure 6: Ablation study of various weighting strategies - Mean, Sum and our ParallelTime Weighter for combining Attention and Mamba outputs.

6.2 Model Efficiency Analysis

Table 2 presents a comparison of MSE and MAE, Floating-Point Operations (FLOPs) for both training and inference and number of parameters, of our model against PatchTST across various prediction lengths using the Traffic dataset. The results show that our model requires significantly fewer FLOPs for both training and inference, achieves higher accuracy, and scales better with larger prediction lengths. This efficiency makes our model particularly well-suited for real-time long-term forecasting applications, where computational resources and speed are critical. For results on additional datasets, refer to Appendix 7.

7 Conclusion and Future Work

In this work, we present ParallelTime, a novel decoder-only architecture that integrates local window attention and Mamba in parallel to effectively capture short-term and long-term dependencies, respectively. The outputs of these components are processed by our innovative ParallelTime Weighter, which adaptively assigns weights to each component for accurate predictions. Our approach achieves state-of-the-art performance across multiple real-world benchmarks while requiring fewer parameters and lower computational costs. This work establishes a foundation for future advancements in parallel Attention-Mamba architectures, poised to enhance long-term time series forecasting.

A key limitation of this study is that, due to limited GPU resources, we could not scale our model to include a large number of layers, which constrained our ability to train on larger datasets or more diverse tasks. Future research can explore the model’s potential as a foundation for time series analysis with minimal adjustments. Specifically, efforts can focus on fine-tuning the model for diverse tasks, such as anomaly detection, classification, and multi-step forecasting, across various domains.

References

Ashish Vaswani, Noam Shazeer, Niki Parmar, Jakob Uszkoreit, Llion Jones, Aidan N. Gomez, Lukasz Kaiser, and Illia Polosukhin. Attention is all you need. In Isabelle Guyon, Ulrike von Luxburg, Samy Bengio, Hanna M. Wallach, Rob Fergus, S. V. N. Vishwanathan, and Roman Garnett, editors, *Advances in Neural Information Processing Systems 30: Annual Conference on Neural Information Processing Systems 2017, December 4-9, 2017, Long Beach, CA*,

- USA, pages 5998–6008, 2017. URL <https://proceedings.neurips.cc/paper/2017/hash/3f5ee243547dee91fbd053c1c4a845aa-Abstract.html>.
- Tom B. Brown, Benjamin Mann, Nick Ryder, Melanie Subbiah, Jared Kaplan, Prafulla Dhariwal, Arvind Neelakantan, Pranav Shyam, Girish Sastry, Amanda Askell, Sandhini Agarwal, Ariel Herbert-Voss, Gretchen Krueger, Tom Henighan, Rewon Child, Aditya Ramesh, Daniel M. Ziegler, Jeffrey Wu, Clemens Winter, Christopher Hesse, Mark Chen, Eric Sigler, Mateusz Litwin, Scott Gray, Benjamin Chess, Jack Clark, Christopher Berner, Sam McCandlish, Alec Radford, Ilya Sutskever, and Dario Amodei. Language models are few-shot learners. In Hugo Larochelle, Marc’Aurelio Ranzato, Raia Hadsell, Maria-Florina Balcan, and Hsuan-Tien Lin, editors, *Advances in Neural Information Processing Systems 33: Annual Conference on Neural Information Processing Systems 2020, NeurIPS 2020, December 6-12, 2020, virtual*, 2020. URL <https://proceedings.neurips.cc/paper/2020/hash/1457c0d6bfc4967418bfb8ac142f64a-Abstract.html>.
- Alexey Dosovitskiy, Lucas Beyer, Alexander Kolesnikov, Dirk Weissenborn, Xiaohua Zhai, Thomas Unterthiner, Mostafa Dehghani, Matthias Minderer, Georg Heigold, Sylvain Gelly, Jakob Uszkoreit, and Neil Houlsby. An image is worth 16x16 words: Transformers for image recognition at scale. In *9th International Conference on Learning Representations, ICLR 2021, Virtual Event, Austria, May 3-7, 2021*. OpenReview.net, 2021. URL <https://openreview.net/forum?id=YicbFdNTTy>.
- Yuqi Nie, Nam H. Nguyen, Phanwadee Sinthong, and Jayant Kalagnanam. A time series is worth 64 words: Long-term forecasting with transformers. In *The Eleventh International Conference on Learning Representations, ICLR 2023, Kigali, Rwanda, May 1-5, 2023*. OpenReview.net, 2023. URL <https://openreview.net/pdf?id=Jbdc0vT0c01>.
- Albert Gu, Karan Goel, and Christopher Ré. Efficiently modeling long sequences with structured state spaces. In *The Tenth International Conference on Learning Representations, ICLR 2022, Virtual Event, April 25-29, 2022*. OpenReview.net, 2022. URL <https://openreview.net/forum?id=uYLFoz1v1AC>.
- Jimmy T. H. Smith, Andrew Warrington, and Scott W. Linderman. Simplified state space layers for sequence modeling. In *The Eleventh International Conference on Learning Representations, ICLR 2023, Kigali, Rwanda, May 1-5, 2023*. OpenReview.net, 2023. URL <https://openreview.net/pdf?id=Ai8Hw3AXqks>.
- Albert Gu and Tri Dao. Mamba: Linear-time sequence modeling with selective state spaces, 2023. URL <https://arxiv.org/abs/2312.00752>.
- Zihan Wang, Fanheng Kong, Shi Feng, Ming Wang, Xiaocui Yang, Han Zhao, Daling Wang, and Yifei Zhang. Is mamba effective for time series forecasting?, 2024. URL <https://arxiv.org/abs/2403.11144>.
- Albert Gu, Tri Dao, Stefano Ermon, Atri Rudra, and Christopher Ré. Hippo: Recurrent memory with optimal polynomial projections. In Hugo Larochelle, Marc’Aurelio Ranzato, Raia Hadsell, Maria-Florina Balcan, and Hsuan-Tien Lin, editors, *Advances in Neural Information Processing Systems 33: Annual Conference on Neural Information Processing Systems 2020, NeurIPS 2020, December 6-12, 2020, virtual*, 2020. URL <https://proceedings.neurips.cc/paper/2020/hash/102f0bb6efb3a6128a3c750dd16729be-Abstract.html>.
- Xin Dong, Yonggan Fu, Shizhe Diao, Wonmin Byeon, Zijia Chen, Ameya Sunil Mahabaleshwar, Shih-Yang Liu, Matthijs Van Keirsbilck, Min-Hung Chen, Yoshi Suhara, Yingyan Lin, Jan Kautz, and Pavlo Molchanov. Hymba: A hybrid-head architecture for small language models, 2024. URL <https://arxiv.org/abs/2411.13676>.
- Haoyi Zhou, Shanghang Zhang, Jieqi Peng, Shuai Zhang, Jianxin Li, Hui Xiong, and Wancai Zhang. Informer: Beyond efficient transformer for long sequence time-series forecasting. In *Thirty-Fifth AAAI Conference on Artificial Intelligence, AAAI 2021, Thirty-Third Conference on Innovative Applications of Artificial Intelligence, IAAI 2021, The Eleventh Symposium on Educational Advances in Artificial Intelligence, EAAI 2021, Virtual Event, February 2-9, 2021*, pages 11106–11115. AAAI Press, 2021. URL <https://ojs.aaai.org/index.php/AAAI/article/view/17325>.

- Tian Zhou, Ziqing Ma, Qingsong Wen, Xue Wang, Liang Sun, and Rong Jin. Fedformer: Frequency enhanced decomposed transformer for long-term series forecasting. In Kamalika Chaudhuri, Stefanie Jegelka, Le Song, Csaba Szepesvári, Gang Niu, and Sivan Sabato, editors, *International Conference on Machine Learning, ICML 2022, 17-23 July 2022, Baltimore, Maryland, USA*, volume 162 of *Proceedings of Machine Learning Research*, pages 27268–27286. PMLR, 2022. URL <https://proceedings.mlr.press/v162/zhou22g.html>.
- Iz Beltagy, Matthew E. Peters, and Arman Cohan. Longformer: The long-document transformer, 2020a. URL <https://arxiv.org/abs/2004.05150>.
- Ze Liu, Yutong Lin, Yue Cao, Han Hu, Yixuan Wei, Zheng Zhang, Stephen Lin, and Baining Guo. Swin transformer: Hierarchical vision transformer using shifted windows. In *2021 IEEE/CVF International Conference on Computer Vision, ICCV 2021, Montreal, QC, Canada, October 10-17, 2021*, pages 9992–10002. IEEE, 2021. doi:10.1109/ICCV48922.2021.00986. URL <https://doi.org/10.1109/ICCV48922.2021.00986>.
- Mikhail S. Burtsev, Yuri Kuratov, Anton Peganov, and Grigory V. Sapunov. Memory transformer, 2020. URL <https://arxiv.org/abs/2006.11527>.
- Timothée Darcet, Maxime Oquab, Julien Mairal, and Piotr Bojanowski. Vision transformers need registers. In *The Twelfth International Conference on Learning Representations, ICLR 2024, Vienna, Austria, May 7-11, 2024*. OpenReview.net, 2024. URL <https://openreview.net/forum?id=2dn03LLiJ1>.
- Roger Waleffe, Wonmin Byeon, Duncan Riach, Brandon Norick, Vijay Korthikanti, Tri Dao, Albert Gu, Ali Hatamizadeh, Sudhakar Singh, Deepak Narayanan, Garvit Kulshreshtha, Vartika Singh, Jared Casper, Jan Kautz, Mohammad Shoeybi, and Bryan Catanzaro. An empirical study of mamba-based language models, 2024. URL <https://arxiv.org/abs/2406.07887>.
- Jamba Team, Barak Lenz, Alan Azaiz, Amir Bergman, Avshalom Manevich, Barak Peleg, Ben Aviram, Chen Almagor, Clara Fridman, Dan Padnos, Daniel Gissin, Daniel Jannai, Dor Muhlgay, Dor Zimberg, Edden M Gerber, Elad Dolev, Eran Krakovsky, Erez Safahi, Erez Schwartz, Gal Cohen, Gal Shachaf, Haim Rozenblum, Hofit Bata, Ido Blass, Inbal Magar, Itay Dalmedigos, Jhonathan Osin, Julie Fadlon, Maria Rozman, Matan Danos, Michael Gokhman, Mor Zusman, Naama Gidron, Nir Ratner, Noam Gat, Noam Rozen, Oded Fried, Ohad Leshno, Omer Antverg, Omri Abend, Opher Lieber, Or Dagan, Orit Cohavi, Raz Alon, Ro'i Belson, Roi Cohen, Rom Gilad, Roman Glozman, Shahar Lev, Shaked Meirum, Tal Delbari, Tal Ness, Tomer Asida, Tom Ben Gal, Tom Braude, Uriya Pumerantz, Yehoshua Cohen, Yonatan Belinkov, Yuval Globerson, Yuval Peleg Levy, and Yoav Shoham. Jamba-1.5: Hybrid transformer-mamba models at scale, 2024. URL <https://arxiv.org/abs/2408.12570>.
- Liliang Ren, Yang Liu, Yadong Lu, Yelong Shen, Chen Liang, and Weizhu Chen. Samba: Simple hybrid state space models for efficient unlimited context language modeling, 2024. URL <https://arxiv.org/abs/2406.07522>.
- Badri N. Patro, Suhas Ranganath, Vinay P. Namboodiri, and Vijay S. Agneeswaran. Heracles: A hybrid ssm-transformer model for high-resolution image and time-series analysis, 2024. URL <https://arxiv.org/abs/2403.18063>.
- Taesung Kim, Jinhee Kim, Yunwon Tae, Cheonbok Park, Jang-Ho Choi, and Jaegul Choo. Reversible instance normalization for accurate time-series forecasting against distribution shift. In *The Tenth International Conference on Learning Representations, ICLR 2022, Virtual Event, April 25-29, 2022*. OpenReview.net, 2022. URL <https://openreview.net/forum?id=cGDAkQo1C0p>.
- Keiron O’Shea and Ryan Nash. An introduction to convolutional neural networks, 2015. URL <https://arxiv.org/abs/1511.08458>.
- Jimmy Lei Ba, Jamie Ryan Kiros, and Geoffrey E. Hinton. Layer normalization, 2016. URL <https://arxiv.org/abs/1607.06450>.
- Kaiming He, Xiangyu Zhang, Shaoqing Ren, and Jian Sun. Deep residual learning for image recognition. In *2016 IEEE Conference on Computer Vision and Pattern Recognition, CVPR 2016, Las Vegas, NV, USA, June 27-30, 2016*, pages 770–778. IEEE Computer Society, 2016. doi:10.1109/CVPR.2016.90. URL <https://doi.org/10.1109/CVPR.2016.90>.

- Iz Beltagy, Matthew E. Peters, and Arman Cohan. Longformer: The long-document transformer, 2020b. URL <https://arxiv.org/abs/2004.05150>.
- Biao Zhang and Rico Sennrich. Root mean square layer normalization. In Hanna M. Wallach, Hugo Larochelle, Alina Beygelzimer, Florence d’Alché-Buc, Emily B. Fox, and Roman Garnett, editors, *Advances in Neural Information Processing Systems 32: Annual Conference on Neural Information Processing Systems 2019, NeurIPS 2019, December 8-14, 2019, Vancouver, BC, Canada*, pages 12360–12371, 2019. URL <https://proceedings.neurips.cc/paper/2019/hash/1e8a19426224ca89e83cef47f1e7f53b-Abstract.html>.
- M.A. Hearst, S.T. Dumais, E. Osuna, J. Platt, and B. Scholkopf. Support vector machines. *IEEE Intelligent Systems and their Applications*, 13(4):18–28, 1998. doi:10.1109/5254.708428.
- Jie Hu, Li Shen, and Gang Sun. Squeeze-and-excitation networks. In *2018 IEEE Conference on Computer Vision and Pattern Recognition, CVPR 2018, Salt Lake City, UT, USA, June 18-22, 2018*, pages 7132–7141. IEEE Computer Society, 2018. doi:10.1109/CVPR.2018.00745. URL http://openaccess.thecvf.com/content_cvpr_2018/html/Hu_Squeeze-and-Excitation_Networks_CVPR_2018_paper.html.
- Peter J. Huber. Robust estimation of a location parameter. In *Breakthroughs in Statistics: Methodology and Distribution*, pages 492–518. Springer, 1992.
- Qingsong Wen, Jingkun Gao, Xiaomin Song, Liang Sun, and Jian Tan. Robusttrend: A huber loss with a combined first and second order difference regularization for time series trend filtering. In Sarit Kraus, editor, *Proceedings of the Twenty-Eighth International Joint Conference on Artificial Intelligence, IJCAI 2019, Macao, China, August 10-16, 2019*, pages 3856–3862. ijcai.org, 2019. doi:10.24963/ijcai.2019/535. URL <https://doi.org/10.24963/ijcai.2019/535>.
- Diederik P. Kingma and Jimmy Ba. Adam: A method for stochastic optimization. In Yoshua Bengio and Yann LeCun, editors, *3rd International Conference on Learning Representations, ICLR 2015, San Diego, CA, USA, May 7-9, 2015, Conference Track Proceedings*, 2015. URL <http://arxiv.org/abs/1412.6980>.
- Ailing Zeng, Muxi Chen, Lei Zhang, and Qiang Xu. Are transformers effective for time series forecasting? In Brian Williams, Yiling Chen, and Jennifer Neville, editors, *Thirty-Seventh AAAI Conference on Artificial Intelligence, AAAI 2023, Thirty-Fifth Conference on Innovative Applications of Artificial Intelligence, IAAI 2023, Thirteenth Symposium on Educational Advances in Artificial Intelligence, EAAI 2023, Washington, DC, USA, February 7-14, 2023*, pages 11121–11128. AAAI Press, 2023. doi:10.1609/AAAI.V37I9.26317. URL <https://doi.org/10.1609/aaai.v37i9.26317>.
- Boris N. Oreshkin, Dmitri Carпов, Nicolas Chapados, and Yoshua Bengio. N-BEATS: neural basis expansion analysis for interpretable time series forecasting. In *8th International Conference on Learning Representations, ICLR 2020, Addis Ababa, Ethiopia, April 26-30, 2020*. OpenReview.net, 2020. URL <https://openreview.net/forum?id=r1ecqn4YwB>.
- Mononito Goswami, Konrad Szafer, Arjun Choudhry, Yifu Cai, Shuo Li, and Artur Dubrawski. MOMENT: A family of open time-series foundation models. In *Forty-first International Conference on Machine Learning, ICML 2024, Vienna, Austria, July 21-27, 2024*. OpenReview.net, 2024. URL <https://openreview.net/forum?id=FVvf69a5rx>.
- Tian Zhou, Peisong Niu, Xue Wang, Liang Sun, and Rong Jin. One fits all: Power general time series analysis by pretrained LM. In Alice Oh, Tristan Naumann, Amir Globerson, Kate Saenko, Moritz Hardt, and Sergey Levine, editors, *Advances in Neural Information Processing Systems 36: Annual Conference on Neural Information Processing Systems 2023, NeurIPS 2023, New Orleans, LA, USA, December 10 - 16, 2023*, 2023. URL http://papers.nips.cc/paper_files/paper/2023/hash/86c17de05579cde52025f9984e6e2ebb-Abstract-Conference.html.
- Haixu Wu, Tengge Hu, Yong Liu, Hang Zhou, Jianmin Wang, and Mingsheng Long. Timesnet: Temporal 2d-variation modeling for general time series analysis. In *The Eleventh International Conference on Learning Representations, ICLR 2023, Kigali, Rwanda, May 1-5, 2023*. OpenReview.net, 2023. URL https://openreview.net/pdf?id=ju_Uqw3840q.

David Campos, Miao Zhang, Bin Yang, Tung Kieu, Chenjuan Guo, and Christian S. Jensen. Lights: Lightweight time series classification with adaptive ensemble distillation. *Proceedings of the ACM on Management of Data*, 1(2), 2023. ISSN 2836-6573. doi:10.1145/3589316. URL <http://dx.doi.org/10.1145/3589316>.

Haixu Wu, Jiehui Xu, Jianmin Wang, and Mingsheng Long. Autoformer: Decomposition transformers with auto-correlation for long-term series forecasting. In Marc’Aurelio Ranzato, Alina Beygelzimer, Yann N. Dauphin, Percy Liang, and Jennifer Wortman Vaughan, editors, *Advances in Neural Information Processing Systems 34: Annual Conference on Neural Information Processing Systems 2021, NeurIPS 2021, December 6-14, 2021, virtual*, pages 22419–22430, 2021. URL <https://proceedings.neurips.cc/paper/2021/hash/bcc0d400288793e8bdcd7c19a8ac0c2b-Abstract.html>.

Yong Liu, Tengge Hu, Haoran Zhang, Haixu Wu, Shiyu Wang, Lintao Ma, and Mingsheng Long. itransformer: Inverted transformers are effective for time series forecasting. In *The Twelfth International Conference on Learning Representations, ICLR 2024, Vienna, Austria, May 7-11, 2024*. OpenReview.net, 2024. URL <https://openreview.net/forum?id=JePFAI8fah>.

8 Appendix

8.1 Dataset

In this study, we assessed the efficacy of our approach by employing seven datasets widely recognized in the domain of long-term time series forecasting: Weather, Traffic, Electricity, Illness, and the ETT datasets (ETTh1, ETTh2, ETTm1, and ETTm2). These datasets encompass a diverse array of periodic patterns and real-world scenarios that present significant predictive challenges, rendering them particularly appropriate for applications such as long-term time series forecasting, data generation, and imputation tasks. A comprehensive description of these datasets is provided in Table 3. The datasets utilized in this research were sourced from [Wu et al., 2021] and [Zhou et al., 2021]

Table 3: Details of multivariate real-world datasets.

Dataset	Variants	Frequency	Timesteps	Information	Forecasting Horizon	Term
Weather	21	10-min	52,696	Weather	(96, 192, 336, 720)	4 years
Electricity	321	Hourly	17,544	Electricity	(96, 192, 336, 720)	2 years
Traffic	862	Hourly	26,304	Road occupancy	(96, 192, 336, 720)	-
Illness	7	-	967	health outcomes	(24, 36, 48, 60)	-
ETTh1	7	Hourly	17,420	electricity transformers	(96, 192, 336, 720)	2 years
ETTh2	7	Hourly	17,420	electricity transformers	(96, 192, 336, 720)	2 years
ETTh1	7	15-min	69,680	electricity transformers	(96, 192, 336, 720)	2 years
ETTh2	7	15-min	69,680	electricity transformers	(96, 192, 336, 720)	2 years

8.2 Training Details and Hyperparameter Settings

8.2.1 Training

All our training was on a single Nvidia RTX 4090,

Efficient Training Strategy. Given the extensive variety in datasets such as Electricity and Traffic, our model encounters memory constraints, even with small batch sizes, on the experimental hardware. Training on high-dimensional multivariate time series, common in real-world applications, is resource-intensive. To mitigate this, we adopt an efficient training strategy inspired by [Liu et al., 2024]. Specifically, we randomly select a subset of variates for each batch, training the model exclusively on these variates to improve efficiency. For the Electricity and Traffic datasets, we use 30 randomly selected variates for the training set and 40 for the validation set, while the test set is used in its entirety.

8.2.2 Hyperparameter settings

We detail the hyperparameters employed in our ParallelTime model for long-term time series forecasting. These include common hyperparameters, applied uniformly across all datasets, and dataset-specific hyperparameters. Common settings include a random seed of 2023 for reproducibility, an input sequence length of 512, Huber loss with a delta of 1.0, attention dropout of 0.1, projection dropout of 0.05, 2 block layers with an attention head size of 4, a patch length of 16, a window attention length of 4, 32 register tokens, and Mamba settings with a state dimension of 16 and convolution dimension of 2. Dataset-specific settings in the table 4.

More Details: We have not explored optimizers beyond Adam. The attention mechanism utilized Flash Attention. We tested Absolute Positional Embedding, Rotary Positional Embedding, and Relative Positional Embedding, with Absolute Positional Embedding performing best.

Table 4: Hyperparameters for the ParallelTime model

Parameter	Electricity	ETTh1	ETTh2	ETTm1	ETTm2	Illness	Traffic	Weather
epochs	20	20	15	30	25	10	25	25
lr	0.005	0.0008	0.0006	0.0001	0.0001	0.012	0.005	0.0004
batch	64	256	512	64	512	64	64	64
dim	128	16	16	32	32	32	128	16

9 Additional results

9.1 Weighting Strategy

This section presents additional results for the weighting strategies applied to Attention and Mamba models, as discussed in Subsection 6.1. The findings demonstrate that, across all prediction lengths and datasets, our ParallelTime Weighter consistently outperforms other weighting strategies, achieving the best results on every dataset.

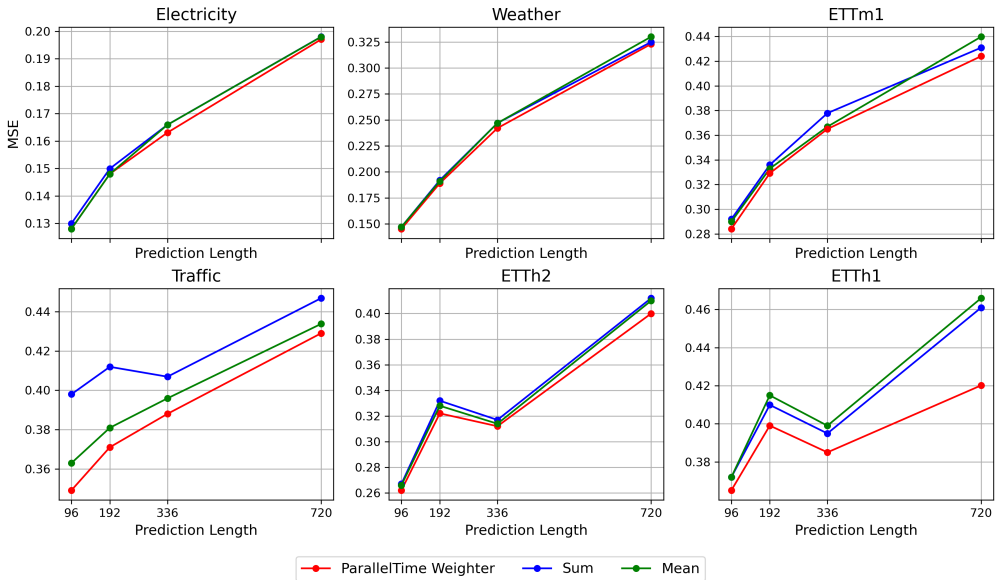


Figure 7: Performance comparison of weighting strategies for Attention and Mamba models across various prediction lengths and datasets, highlighting the superior results of our ParallelTime Weighter.

9.2 Study of Expand-Compress-Project

In this subsection, we present a comparative analysis of our proposed Expand-Compress-Project method against the standard projection method in time series forecasting. Table 5 provides a detailed comparison across various datasets and prediction lengths. It is evident from the table that the our Expand-Compress-Project method consistently achieves similar and sometimes better MSE values to the standard projection method while significantly reduces the number of parameters required, in addition we can see that our model scale better on larger sequence length.

Table 5: Comparison of Expand-Compress-Project and Standard Projection Methods for different prediction lengths, where our method utilizes significantly fewer parameters while maintaining similar accuracy

Dataset		MSE		#params	
		Expand-Compress	Standard Projection	Standard Projection	Expand-Compress
Electricity	96	0.128	0.127	854.432 K	516 K
	192	0.148	0.146	1.2477 M	552.96 K
	336	0.163	0.162	1.8377 M	608.4 K
	720	0.197	0.196	3.411 M	756.24 K
Traffic	96	0.349	0.353	953.248 K	614.816 K
	192	0.371	0.372	1.3466 M	651.776 K
	336	0.389	0.389	1.9365 M	707.216 K
	720	0.430	0.432	3.5098 M	855.056 K

9.3 Patch-Level Weight Additional Analysis

We visualize a sample from the ETTM1 dataset to illustrate the distribution of short-term and long-term dependencies utilized by our model for each token (patch). We extract the weights assigned by our ParallelTime Weighter and present them in Figure 8. The visualization reveals that patches significantly different from preceding patches (from left to right) rely more heavily on the Mamba weights, which emphasize long-term dependencies. Conversely, when the data exhibits minimal variation, greater weight is assigned to window attention, which prioritizes short-term dependencies. Additionally, we observe distinct behaviors across different layers.

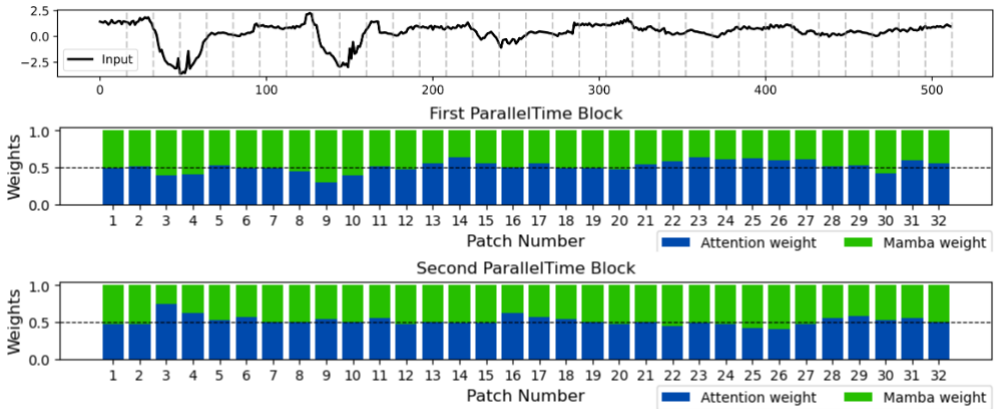


Figure 8: Visualization of input series and the weight distribution per patch in sample from ETTM1 dataset, for the first and second ParallelTime blocks.

9.4 Robustness

Effects of Different Parameter Adjustments. To evaluate the impact of hyperparameter choices on ParallelTime, we conducted additional experiments by adjusting key model parameters. We tested different configurations by varying the number of ParallelTime layers, $L = 1, 2, 3$, and the patch size, $P = 8, 16$, resulting in a total of six unique hyperparameter combinations. The MSE scores for these configurations across various datasets are presented in Figure 9. Most datasets show consistent performance across hyperparameter settings, except for the ILI dataset, which exhibits slightly variable results.

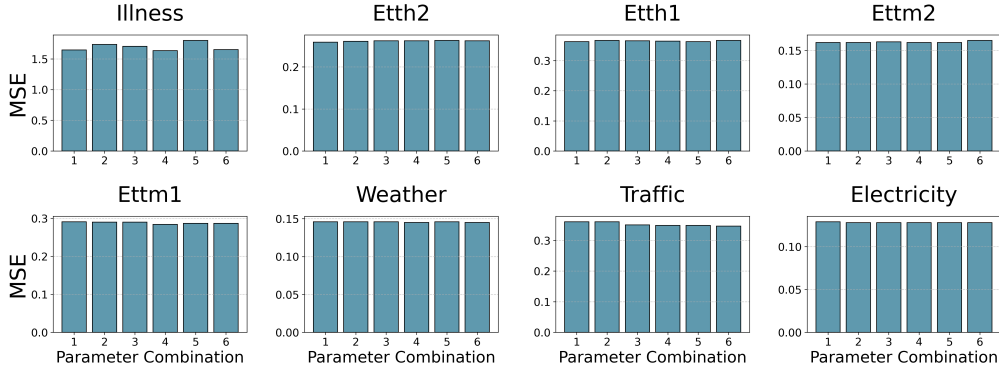


Figure 9: MSE scores for ParallelTime across six hyperparameter configurations (number of layers $L = 1, 2, 3$, patch size $P = 8, 16$).

Dataset	ETTh2		Traffic		Weather	
Horizon	MSE	MAE	MSE	MAE	MSE	MAE
96	0.263±0.0011	0.328±0.0007	0.350±0.0009	0.231±0.0000	0.146±0.0007	0.190±0.0011
192	0.323±0.0011	0.368±0.0013	0.371±0.0000	0.241±0.0005	0.191±0.0011	0.234±0.0011
336	0.313±0.0008	0.371±0.0013	0.390±0.0012	0.252±0.0011	0.244±0.0015	0.276±0.0015
720	0.404±0.0036	0.437±0.0027	0.429±0.0009	0.274±0.0004	0.324±0.0026	0.331±0.0015

Dataset	ETTm1		ETTm2		Electricity	
Horizon	MSE	MAE	MSE	MAE	MSE	MAE
96	0.289±0.0036	0.341±0.0035	0.162±0.0004	0.252±0.0004	0.128±0.0004	0.222±0.0004
192	0.330±0.0019	0.368±0.0021	0.221±0.0029	0.292±0.0016	0.147±0.0005	0.240±0.0015
336	0.361±0.0025	0.389±0.0012	0.276±0.0023	0.327±0.0011	0.164±0.0008	0.258±0.0004
720	0.436±0.0085	0.434±0.0034	0.356±0.0046	0.380±0.0022	0.197±0.0008	0.288±0.0010

Table 6: Robustness from five different random seeds.

Impact of Various Random Seeds. The findings presented in the main text and appendix were obtained using a consistent random seed of 2023. To assess the stability of these outcomes, we trained the supervised ParallelTime model using five random seeds: 2022, 2023, 2024, 2025, and 2026, computing the MSE and MAE scores for each seed. The average and standard deviation of these results are shown in Table 9.4. The notably low standard deviations demonstrate that our model’s performance remains stable across different random seed selections.

Dataset	Pred Len	MSE		MAE		Fwd FLOPs		Fwd+Bwd FLOPs		#Params	
		ParallelTime	PatchTST	ParallelTime	PatchTST	ParallelTime	PatchTST	ParallelTime	PatchTST	ParallelTime	PatchTST
ETTh1	96	0.365 (↓1.4%)	0.370	0.398 (↓0.3%)	0.399	0.325G (↓52%)	0.687G	0.976G (↓52%)	2.062G	69k (↓40%)	116k
	192	0.399 (↓3.4%)	0.413	0.415 (↓1.4%)	0.421	0.347G (↓52%)	0.731G	1.042G (↓52%)	2.194G	119k (↓44%)	214k
	336	0.385 (↓8.8%)	0.422	0.414 (↓5.0%)	0.436	0.380G (↓52%)	0.797G	1.141G (↓52%)	2.392G	192k (↓46%)	362k
	720	0.420 (↓6.0%)	0.447	0.443 (↓4.9%)	0.466	0.468G (↓51%)	0.973G	1.405G (↓51%)	2.920G	389k (↓48%)	755k
Electricity	96	0.128 (↓0.8%)	0.129	0.222	0.222	7.00G (↓47%)	13.2G	21.0G (↓47%)	39.5G	516k (↓57%)	1194k
	192	0.148 (↓5.7%)	0.157	0.241	0.240	7.02G (↓48%)	13.5G	21.1G (↓48%)	40.6G	553k (↓72%)	1981k
	336	0.163	0.163	0.258 (↓0.4%)	0.259	7.04G (↓50%)	14.1G	21.1G (↓50%)	42.2G	608k (↓81%)	3161k
	720	0.196 (↓0.5%)	0.197	0.288 (↓0.7%)	0.290	7.11G (↓54%)	15.5G	21.3G (↓54%)	46.4G	756k (↓88%)	6307k

Table 7: Comparison of ParallelTime and PatchTST on ETTh1 and Electricity datasets. The table reports MSE, MAE, forward (Fwd) FLOPs (i.e., inference FLOPs), forward and backward (Fwd+Bwd) FLOPs (i.e., training FLOPs), and the number of parameters (#Params) for different prediction lengths (Pred Len).